国際化推進共同研究概要

No. 1

タイトル: Effects of tansmutant helium on the microstructure of fusion reactor structural materials.

研究代表者: ODETTE, George, Robert

所内世話人: 渡辺 英雄

実 施 期 間: 2013 年 6 月 19 日～ 6 月 30 日

研究概要: 融合炉及び先進炉材料としての使用が期待される鉄系構造材料の照射環境下での脆化挙動解明を目的として、ヘリウム注入下でのイオン並びに電子線照射を炉の使用温度にて実施した。TEM(九大)及びアトムポローブ(UCSB)による観察から、銅クラスターや微小バブルの双方が照射による脆化には大きな役割を占めることが明らかにされた。

Effects of transmutant helium and displacement damage on the microstructure of fusion and fission reactor structural materials

Takuya Yamamoto, Yuan Wu, Peter Wells, G. Robert Odette (University of California Santa Barbara), Hideo Watanabe, Takahiro Onishi (Kyushu University)

Introduction

One of the challenges that fusion reactor materials development faces is to manage and mitigate the possible effects of transmutation He on the mechanical properties of first wall structural materials. One year operation of a typical DEMO reactor would produce ≈ 500 appm He along with the displacement damage of ≈ 50 dpa. Helium bubbles form in the matrix as well as on dislocations, precipitate interfaces and grain boundaries (GB) [1]. Recent experiments in HFIR reactor using in situ He implanter (ISHI) technique have shown that in TMS F82H and Eurofer 97 distinct bi-modal cavity size distributions develop even at ≈ 10 dpa and ≈ 400 appm He, that consists of numerous small bubbles with average diameter of ≈ 2 nm and fewer large faceted cavities, which are likely voids [2]. The voids can nucleate at bubbles that have reached a critical size, then continuously grow increasing the volume fraction of cavities, corresponding to void-swelling, to ≈ 0.5% at 21 dpa [3]. Such He-dpa synergistic effects on the swelling that is life-limiting factor in the intermediate temperature range has to be understood and modeled accurately to predict the structure's performance during the fusion reactor operation, along with the low temperature embrittlement and high temperature creep behavior. The objective of this research is to study microstructural evolution in the materials under charged particle irradiations at various combinations of He and dpa. For example, He ion irradiation in High energy ion generating apparatus (HEIGA) at RIAM would produce very high He to dpa ratio, while High voltage electron microscope (HVEM) allows in-situ observation of microstructural evolution of previously introduced He bubbles while 1 MeV electrons additionally introduce dpa damages. We compare the results with our other irradiation experiments including ISHI and dual ion beam irradiation experiments to understand combined effects of the irradiation variables.

At the same time, the effects of characteristic differences between the irradiation techniques on microstructural evolution must be well understood in order to properly interpret the experimental results. The electron beam irradiations create only Frenkel (vacancy and self interstitial atom) pairs, while cascade effects are expected to be important under ion beam irradiations. Defect survival is expected to be higher for electrons, while intra cascade clustering occurs in aged cascades. Here we have chosen RPV alloys with a range of Cu and Ni contents as target materials for the study. Formation of Cu-rich and Mn-Ni-Si precipitates under ion irradiations as well as neutron irradiations have been characterized at UCSB for those alloys. Electron beam irradiations are carried out to study the microstructural evolutions under simple Frenkel pair production as opposed to cascade damages in ion or neutron irradiations.

Experimental procedure

Since He ion source is not available in HEIGA this year, we focused on HVEM experiments. F82H specimen irradiated up to nominal ≈ 26 dpa and ≈ 1230 appm He at 500 °C in dual (Fe^{3+} and He^{+}) ion beams in the DuET facility at Kyoto University was observed under 1 MeV electron beam irradiation in HVEM. Typically 5μm wide, 2.5 μm deep and 150 nm thick samples were lifted out of the dual ion beam irradiated F82H TEM discs using FIB (Focus Ion-beam) micro-machining. TEM microstructures were observed at UCSB using FEI Technai microscope before and after the electron irradiation as well as in situ HVEM observations at 500°C.

Electron beam irradiations were also carried out on a 0.2Cu-0.8Ni-1.4Mn-0.5Si model RPV steel. Mechanical and electro-polishings and FIB machining were employed to prepare HVEM transparent sample with a rectangular notch as a landmark for target location as shown in Figure 1. Two irradiations to the displacement damages of 0.1 and 0.4 dpa were carried out at a temperature of 290°C and a damage rate of 2.5 x 10^{-5} dpa/s for the locations indicated in Fig.1. Size of the irradiated regions is about 9 μm in diameter and the thickness of about 200 nm. TEM observations and atomprobe tomography (APT) have been carried out for the irradiated region. Steps of FIB machining were also employed to prepare APT samples from the irradiated regions.

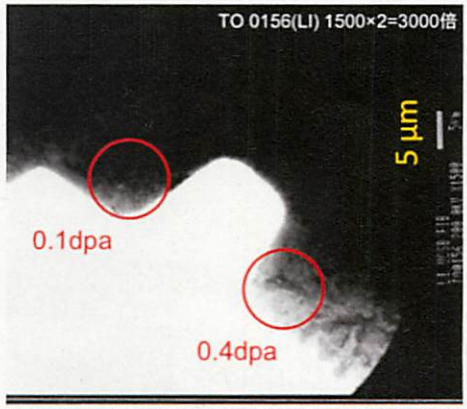

Figure 1 Electron irradiated regions near the FIB machined landmark in a 0.2Cu-0.8Ni-1.4Mn-0.5Si model steel specimen.

Results

Figure 2 shows an example of cavity microstructure in the F82H specimen after the nominal 26 dpa & 1230 appm He DuET irradiation, taken at ≈ 1 μm from the surface, corresponding to an estimated 42 dpa and 2100 appm He. A moderate number density (N ≈ 2.6 ± 0.3 x 10^{22} m^{-3}) of cavities distributed over a wide range of diameters (d), from ≈ 1 nm (bubbles) up to > 20 nm (voids). A few attempts of electron beam irradiation at 500°C resulted in a significant Cu contamination over various parts of the specimens, which may be due to local temperature excursion of the specimen mount made of Cu. This did not occur when a low dose DuET F82H specimen was irradiated previously in a similar manner. Exact cause of the Cu contamination is yet to determine, while further HVEM attempts with improved beam heat transfer are being prepared.

Figure 3 shows examples of APT solute atom distributions in 0.2Cu-0.8Ni-1.4Mn-0.5Si RPV alloy after electron irradiations to (a) 0.1 and (b) 0.4 dpa, respectively, compared with corresponding Fe^{3+} ion and neutron irradiations. At the lower dose, Cu clusters are observed in electron irradiation that are far smaller and less enriched in Mn-Ni-Si than for corresponding ion and neutron irradiations. The differences are much larger even at lower dpa in the case of low dose rate neutron irradiations. However, once formed the Cu rich precipitates grow very rapidly under electron irradiation to larger volume fraction at 0.4 dpa than in the case of ions at 1 dpa. This growth is primarily associated with addition of Mn-Ni-Si solutes, which dominate the precipitate compositions and that are similar to those in ion and neutron irradiations at 1.7 dpa. However, the precipitates are smaller and more numerous in electron irradiation compared to ion or neutron irradiations. TEM shows that loops are only observed at 0.4 dpa in electron irradiation. These results suggest that cascades and, perhaps, loops play a role in precipitate evolution.

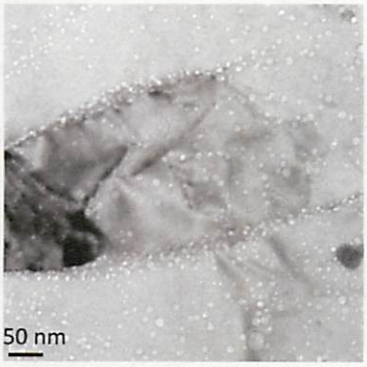

Figure 2 Cavity microstructure in F82H irradiated to nomial 26 dpa and 1210 appm He at 500°C.

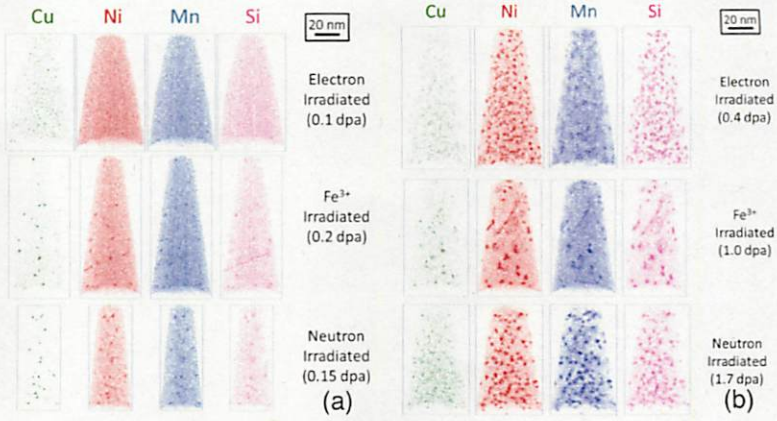

Figure 3 APT Solute atom distributions in a 0.2Cu-0.8Ni-1.4Mn-0.5Si RPV alloy electron irradiated to (a) 0.1 dpa and (b) 0.4 dpa, compared with a corresponding damage levels in Fe^{3+} ion or neutron irradiations.

Summary

We have performed 1 MeV electron beam irradiation for tempered martensitic steel F82H previously irradiated to nominal 26 dpa with 1230 appm He at 500°C in DuET dual ion beam facility at Kyoto University. A few HVEM attempts resulted in anomaly Cu contaminations over the specimens possibly due to specimen temperature excursions. Further attempts will be made with improving sample mount with better heat transfer. Electron irradiations for a 0.2Cu-0.8Ni-1.4Mn-0.5Si RPV alloy showed slower nucleation of Cu-rich precipitates but faster growth of them to a volume fraction larger than corresponding ion or similar to neutron irradiations, associated with addition of Mn-Ni-Si solutes. The precipitates are smaller and more numerous in electron irradiation compared to ion or neutron irradiations. These and similar timing of loop growth suggest that cascades and, perhaps, loops play a role in precipitate evolution.

Acknowledgements

Authors are grateful to Professor Akihiko Kimura and Dr. Sosuke Kondo at Kyoto University for DuET irradiation. Part of the research performed by UC Santa Barbara participants is supported by US DOE.

References:

1. Y. Dai, G. R. Odettte, T. Yamamoto, *The Effects of helium on irradiated structural alloys* in: R.J.M. Konings(ed.) Comprehensive Nuclear Materials, volume 1, pp. 141-193 Amsterdam: Elsevier (2012)
2. T. Yamamoto, G.R. Odette, P. Miao, D. J. Edwards, R. J. Kurtz, J. Nucl. Mater., 386-388 (2009) 338.
3. G.R. Odette, P. Miao, D.J. Edwards, T. Yamamoto, R.J. Kurtz, H. Tanigawa, J. Nucl. Mat. 417 (2011) 1001.
4. G.R. Odette, M.J. Alinger, and B.D.Wirth, Annu. Rev. Mater. Res. 38 (2008)471.

国際化推進共同研究概要

No. 2

タイトル: Towards high mode purity in ECRH transmission lines for ITER.

研究代表者: KASPAREK, Walter, Hermann

所内世話人: 出射 浩

実 施 期 間: 2014 年 3 月 23 日 ～ 3 月 29 日

研究概要: A. Zach

W. Kasparek との共同研究課題で3月23日から29日の予定で来所する予定である。今年度、新モード分析器と高速伝送路切り替えのための分波器、2つの課題を議論する。新モード分析器は不要モードが高次ベッセル関数に振幅を持つことに着目して開発が進められている。大電力伝送路でのモード分析のため、サンプルするための結合度を低く設計されており、低電力試験でのダイナミックレンジ等を議論する。分波器は方形コルゲート導波管を用いるタイプを開発している。コルゲート溝形状が与える抵抗損、伝搬位相への影響等、高周波動作を議論する。

Towards high mode purity in ECRH transmission lines for ITER

Applicant: Walter Kasparek

Institute of Interfacial Process Engineering and Plasma Technology (IGVP)

The work performed under support of the Collaborative Research Program of the Research Institute for Applied Mechanics, Kyushu University, dealt with methods to characterize oversized corrugated transmission lines and to increase the performance of launchers in high-power ECRH systems.

The International Joint Research team consisted (besides the applicant) of Hiroshi Idei (RIAM, Kyushu), Keishi Sakamoto (JAEA Naka), Takashi Shimozuma (NIFS, Toki), Richard Temkin (MIT PSFC Cambridge), Michael Shapiro (MIT PSFC Cambridge), Carsten Lechte (IGVP Stuttgart), and Burkhard Plaum (IGVP Stuttgart).

Mode Contents Monitor Development

In last year, a new type of mode contents monitor was proposed to analyze the transmitted mode structure in oversized corrugated circular (CC) waveguide (WG). The unwanted modes have higher-mode Bessel functional amplitude, and +/- turning points (nulls) of the amplitude distributions with phase jumps of π. Coupling structures with appropriate positioning in the surface of the mitre bend mirrors allows detection of these modes. Here, a key issue is the 0/π – phasing of the Waveguide couplers.

The 0/π –phasing WG coupler has been designed and fabricated. First we checked its performance in the low power test. A narrow beam radiated from a corrugated horn antenna was directly injected to a circular CC WG. HE1n (mainly HE13) modes were excited at the coupling into the WG.

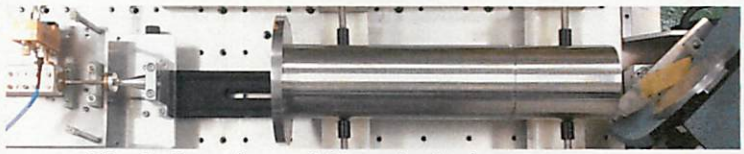

Fig. 1: Experimental Setup in the low power test

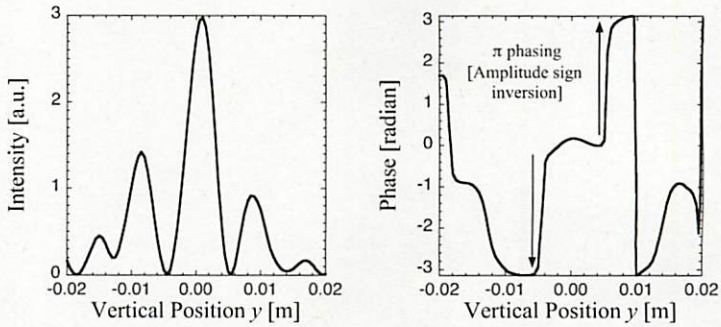

Fig. 2: Field distribution radiated from CC WG after the coupling.

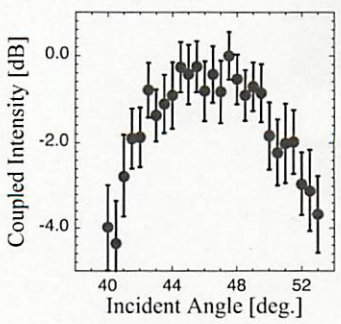

Fig. 3: 0-phasing WG coupler performance depending on the incident angle

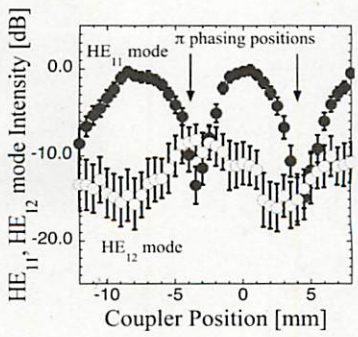

Fig.4: 0/□π - phasing WG coupler performances in scanning of coupler position

Figure 1 shows the experimental setup to excite the beam with the HE1n modes after the coupling. The radiated field distribution was measured as shown in Fig. 2. We had the +/- turning points of the amplitude distributions with the π - phasing in the higher-mode Bessel functional amplitude. Basic 0 - phasing WG coupler performance was checked in dependence of the coupling on incident angle as shown in Fig. 3. Maximum coupling was observed around the 45 degree incident angle, and it was confirmed to work properly. The 0/π -phasing WG coupler performances were checked in scanning of WG coupler positions for the beam radiated from the CC WG with the +/- turning points. The smaller and larger couplings were observed the 0/π -phasing WG couplers around the +/- turning points. The 0/π -phasing WG coupler performances worked correctly. Main problems were the dynamic range or S/N in the low power test, coming from low level coupling at the coupling hole-array (~ -60dB).

The high power test has been conducted at JAEA. First the 0-phasing WG coupler performance was checked in scanning of incident polarizations. Two orthogonal E_x and E_y components were clearly distinguished by specific WG couplers respectively, indicating low stray radiation components in the measurements as shown in Fig. 5. In the high power test, we had a HE12 (LP02) mode as a second dominant mode (~3%). The HE21 and HE13 (LP03) modes were less (<~1%). We could measure only the HE12 (LP02) components by the π-phasing WG coupler as shown in Fig. 6. The other modes were not measured, showing low cross talk for the main HE11 mode.As the next step, we are going to conduct the low and high power tests under incident angle control to excite the HE21 mode.

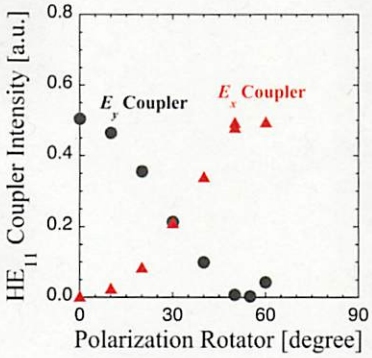

Fig. 5: Two orthogonal E_x and E_y components measured by specific WG couplers

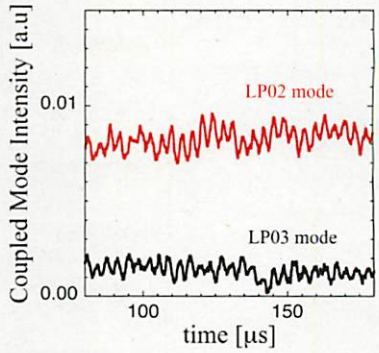

Fig. 6: LP02 and LP03 modes detected at the π - phasing WG coupler

In support of the developments on mode analyzers at RIAM, Kyushu University, calculations and experiments on low-power mock-ups for 5-port couplers have been performed, using the tracer modes for misalignment (LP11,odd and LP11,even) and beam mismatch (LP02) as well as the main transmission mode (LP01). Here, a slightly different concept was used, which is based on amplitude (including phase) measurements of the signals from various couplers. The mode amplitudes are obtained as the weighted averages of the complex field amplitudes. Low-power measurements confirm the calculations, but show limited accuracy due to phase and amplitude errors due to insufficient dynamic range of the measurement system (Fig. 7, right). The presence of higher-order modes will also reduce the precision, as was shown by calculations (see Fig. 7, left). Moreover, calibration of the couplers was an issue. Note that in this context, high-purity mode generators are developed (see below).

For the generation of various modes for the coupler tests, a new resonator, which uses the wanted mode field as an eigenmode, was designed and built. It consists of two mirrors, an exchangeable phase-reversing mirror designed for the LP01, LP02, or LP11 mode field, which is defined according to the waveguide parameters on the interface plane between resonator and waveguide, and a semi-transparent plane mirror as output coupler. The excitation of the resonator was performed via a beam splitter and a Gaussian feed horn. Up to

now, detailed measurements of amplitude and phase of the output fields, and evaluation of the efficiency and mode purity have been performed for the LP01 resonator.

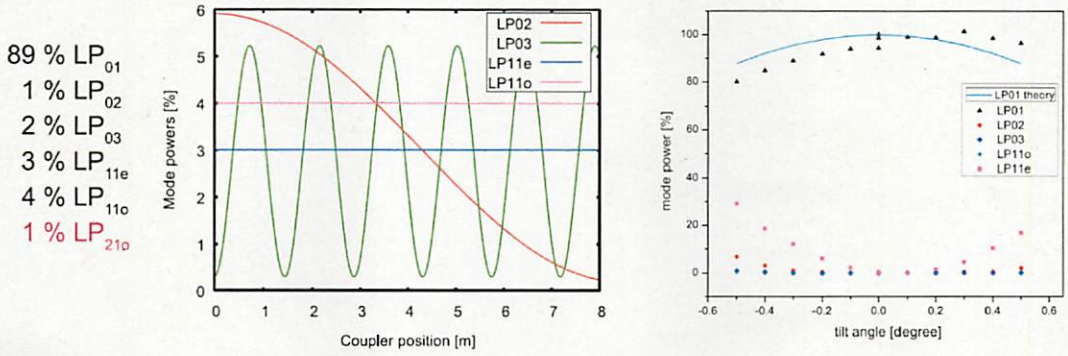

Fig. 7, left: Theoretical results showing that a 1% presence of a sixth mode spoils the results for all symmetric modes, i.e. leading to a dependence of the signal on the coupler position. Right: Measurements of the higher order mode content caused by a known tilt in the waveguide.

So far, a rather good LP01 mode was generated, having a purity of > 98 % (Fig. 8). Tests with the other modes are to follow. As a preliminary conclusion of this mode generator concept, we can state, that a perfect output mode can be reached for a good matching of the exciting beam with the resonator mode, avoidance of any interference with the excitation beam, and a precise semi-transparent mirror with all 1700 coupling holes being identical. For mode purities of > 99 %, this would require a refurbishing of the present design.

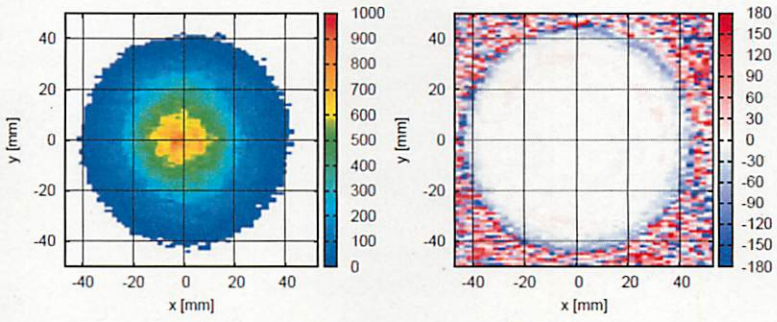

Fig. 8: Measured output field amplitude distribution (left and Phase profil (right) for the LP01 mode generator at 140 GHz. The mode purity calculated from the overlap integral between theory and measurement is 98.06 %

2-frequency (110/138 GHz) FADIS

FADIS has been developed to switch fast the transmission lines of ECH/ECCD experiments by using the steep slopes in the transmission characteristic together with frequency-shift keying of gyrotrons. The local current driven by ECCD has been in operation to suppress NTM mode activities in the tokamak. Synchronous switching for the mode rotation using the FADIS was proposed for more effective suppression. A 2-resonant-ring system with square corrugated (SC) WG splitter was proposed for the FADIS in a 2-frequency gyrotron system. The conceptual design of the SC WG splitter was finished, and engineering design has been begun under this collaboration framework.

I. Corrugated Structure

A normal rectangular corrugation has large Ohmic losses depending on incident polarization for large incident angle into the SC WG splitter. A Gaussian corrugated structure was proposed to reduce the Ohmic loss. Wave phase reflected at the corrugated plane was calculated with a moment method simulator to design Gaussian-corrugation height and pitch. Optimized height and pitch of the Gaussian corrugation were 0.68 mm and 1 mm.

II. Cu Electroforming

Electroforming was considered as an attractive fabrication technique. Copper was proposed as electroforming material, and some materials have been considered as its mold. Aluminum molds are easy to fabricate, but it will be destroyed after the electroforming. Reusable SUS and glass have been considered as the mold materials, and its fabrication process has been reviewed. For a slightly scaled frequency of 140 GHz, a study, prototype fabrication, and testing of a SC WG using Aluminium molds was performed. To ease the fabrication, a set of slightly modified Gaussian-type corrugations was used.

III. Prototype testing

Up to now, various 20 cm long test samples of corrugated waveguide were produced, and their performance was tested using a 3-mirror resonator. This device allows an accurate measurement of the ohmic losses occurring upon reflection of the waves from the waveguide wall; from this information, the ohmic loss of the complete SC splitter WG can be deduced. Moreover, the phase shift of the wall between the polarization component parallel (TE, or H-plane) and perpendicular (TM, or E-plane) to the grooves can be measured very precisely. Thus, a complete characterization of the waveguide as function of the angle under which the waveguide is operated, can be performed. The result for the best performing corrugation is given in Fig. 9.

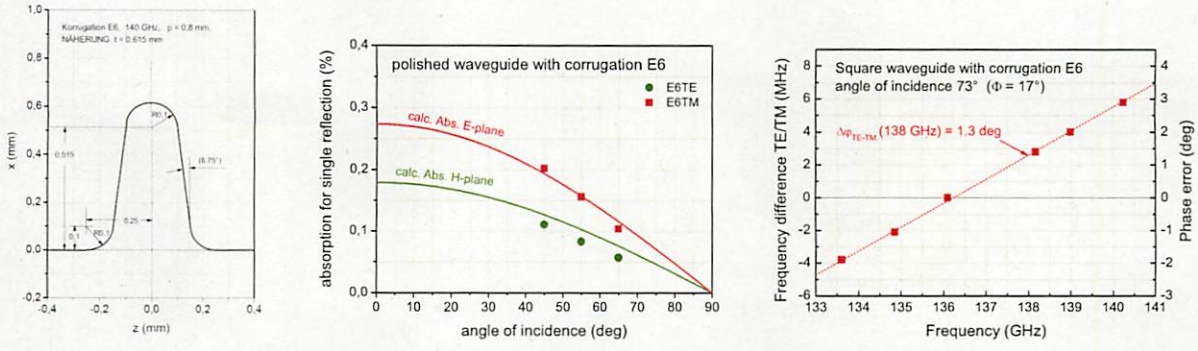

Fig. 9: Left: Profile of corrugation. Middle: absorption of the corrugated waveguide wall for one reflection as function of the angle of incidence and E- and H polarization; solid lines: calculation, symbols: measurements. Right: phase shift between E- and H-polarization for angle of incidence of 73 deg, as a function of frequency. Note that at f = 138 GHz, a phase error of only 1.3 deg is obtained.

国際化推進共同研究概要

No. 3

タイトル: Joint study of confinement plasma on different divertor plasma shape and related egde turbulence transport in steady state operation (SSO) plasmas on QUEST and EAST.

研究代表者: GAO, Xiang

所内世話人: 花田 和明

実 施 期 間: 2014 年 2 月 16 日 ～ 2 月 23 日

研 究 概 要: 今年度は2名の学生を ASIPP に派遣し、硬 X 線計測と Li ペレットに関するデータを解析して発表を行なった。また、2月16日－23日の日程で来所し、昨年度発表した論文に続いて高速度カメラによる Blob の観測を行いデータの整理を行った。中国で検討している次期装置に関する講演を実施して中国で進めている核融合研究の現状と課題について議論を行った。

RESEARCH REPORT

Date Mar. 5, 2014

Visiting scientists: (name) Xiang Gao

(position) Professor

(university / institute) Institute of Plasma Physics,
Chinese Academy of Sciences

(name) Haiqing Liu

(position) Associate Professor

(university / institute) Institute of Plasma Physics,
Chinese Academy of Sciences

(name) Zhengxing Wang

(position) Master student

(university / institute) Institute of Plasma Physics,
Chinese Academy of Sciences

Host scientist: (name) Kazuaki Hanada

(position) Professor

(university / institute) Kyushu University

Research period: (from) Feb. 16, 2014 (to) Feb.22, 2014

Research subject: **Joint study of confinement plasma on different divertor plasma shape and related egde turbulence transport in steady state operation (SSO) plasmas on QUEST and EAST**

The mission of QUEST is to develop the scientific basis for achieving a steady state condition at sufficiently high beta (~20%), with high confinement and low collisionality. In spherical tokamaks (STs), a further development on divertor geometry is required because of their compactness. Therefore, in QUEST, some special types of divertor geometry and configurations can be explored and applied, as well as snowflake in NSTX and super X in MAST-U. The mission of the EAST project is to study the physical issues involved in steady state advanced tokamak devices. EAST has a flexible poloidal field control system to accommodate both single null(SN) and double-null (DN) divertor configurations. ITER-like divertor geometry and target structure has adopted to minimize the leakage of neutrals to the main chamber. Joint study confinement plasma on different divertor plasma shape in SSO plasma research field on QUEST and EAST is aiming to contribute to the ITER project. In addition, edge turbulence (blobs, filaments, ELMs etc) transport plays an important role in high confinement plasma with SSO. In QUEST, the combination diagnostics of radial probe(Langmuir probe in mid-plane), divertor probes and fast camera is a powerful tool to study the edge turbulence (blobs, filaments) transport. In EAST, type I and type III ELMs and filaments has been observed in H-mode and L-mode in SSO discharges. Joint study of edge turbulence transport on QUEST and EAST will provide some key understandings on confinement improvement.

In this one week international joint research, progress on steady state operation (SSO) plasmas on QUEST and EAST was discussed. Prof. Gao present "Update on CFETR Concept Design" and EAST 30s long pulse discharges. New blobs experiment in slab plasma on QUEST was observed with new photron fast camera.

On EAST tokamak, we demonstrate a high-confinement plasma regime known as an H-mode with a record pulse length of over 30 s in the Experimental Advanced Superconducting Tokamak sustained by lower hybrid wave current drive (LHCD) with advanced lithium wall conditioning, as shown in fig.1. We find that LHCD provides a flexible boundary control for a ubiquitous edge instability in H-mode plasmas known as an edge-localized mode, which leads to a marked reduction in the heat load on the vessel wall

compared with standard edge-localized modes. LHCD also induces edge plasma ergodization that broadens the heat deposition footprint. The heat transport caused by this ergodization can be actively controlled by regulating the edge plasma conditions. This potentially offers a new means for heat-flux control, which is a key issue for next-step fusion development.

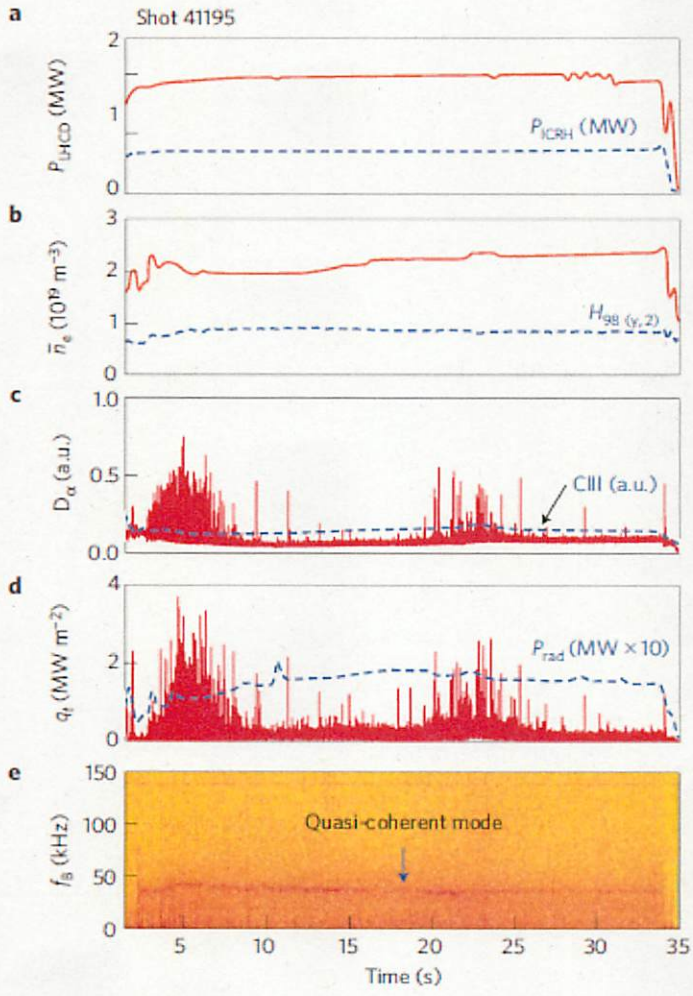

Fig. 1 An H-mode with a record pulse length of over 30 s on EAST sustained by LHCD (J.Li *et al.*, Nature physics)

Non inductive current drive is more important for QUEST because not enough space in center part to put coils in case of spherical tokmak. Using electron cyclotron resonance current drive(2Ωe-ECCD) is one of the powerful method on QUEST. In QUEST, it was succeeded to drive current Ip=30 kA using 8.2GHz fundamental wave ECCD. Higher frequency 28GHz gyrotron was introduced, 2nd harmonic ECCD was used and non

inductive plasma current reached Ip=60kA. An Ip=30kA discharges sustained by 28 GHz and 8.2 GHz ECCD on QUEST is shown in Fig.2.

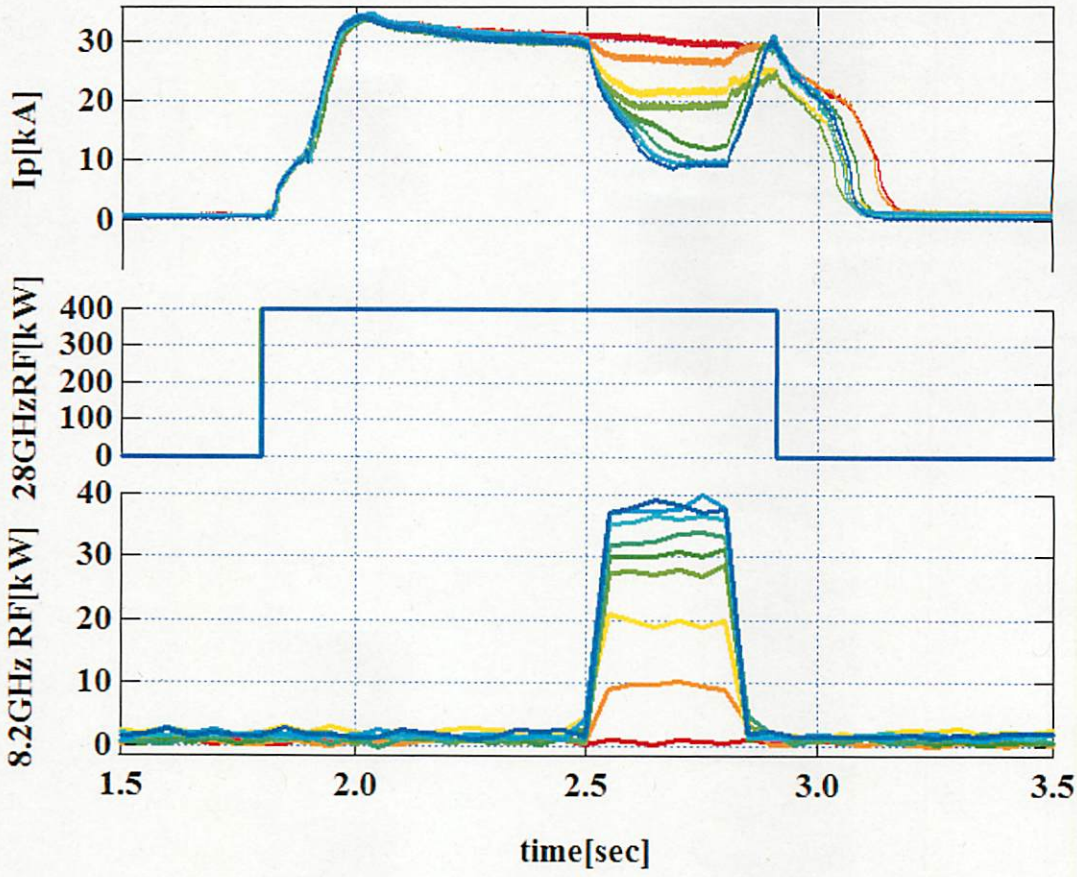

Fig.2 An Ip=30kA discharges sustained by 28 GHz and 8.2 GHz ECCD on QUEST (Mr. Suzukawa's presentation)

The China Fusion Engineering Test Reactor(CFETR) concept design was fulfilled in last three years. The goal of CFETR is to bridge the gap between ITER and DEMO and to realize the fusion energy in China. Concept design of CFETR which includes: full superconducting magnets and water cooling Cu magnets is well progressing, as shown in Fig.3. The engineering parameters of the device have been determined by considering engineering constraints. The two design options will be finished by Sept. 2014. CFETR operation modes have been studied. SSO is proved to be possible. More detailed 1.5D calculation needs to be done. A new design of large vertical window scheme was selected by discussing the advantages and disadvantages of the three conceptual CFETR design.

ITER-like, snowflake, super-X divertor configurations have been studied. Integration design of divertors for ITER-like and snowflake configurations has been done. Many upgrades on EAST tokamak have been developed towards CFETR R&D items recently.

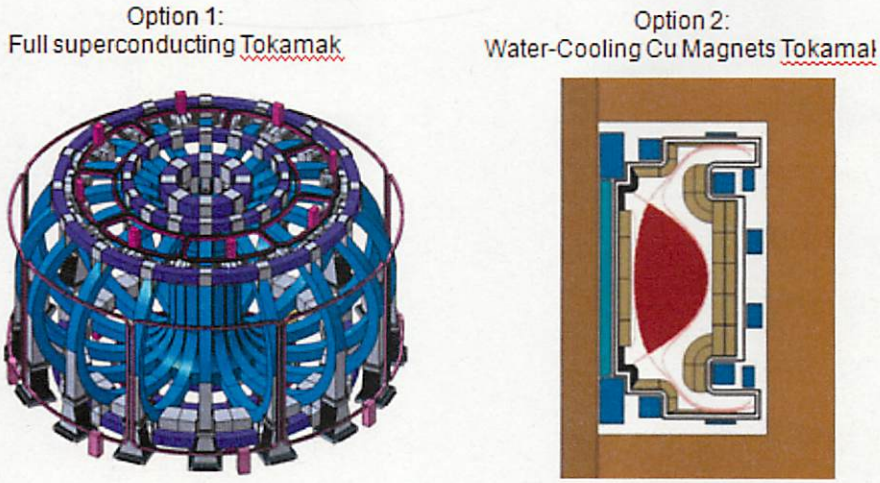

Fig. 3 Two options of CFETR(Prof. Gao's presentation)

Blob causes huge amount of energy and particle losses. Blobs' characteristics are not yet well understood because of its complicated nature. In particular for fusion, is further amplified by similarities between blobs and ELM filaments, which suggest that the same mechanism is governing their dynamics. Recent measurements reveal parallel currents associated with filaments during ELMs, which result in large net currents to divertor plates. The importance of parallel currents on blob propagation could be inferred by comparing experimental blob speed-versus-size scalings with theory predictions. The existence of two regimes for blob propagation, in which parallel currents to the sheath, respectively, do or do not efficiently damp the gradB and curvature induced polarization of the blob. Connection length is important due the existence of sheath connection, in which the sheath do significantly damp charge separation and thus blob radial velocity. When the pitch of a blob-like structure is shortened, the return current may flow between the pitch. The threshold is unclear now. For blob research, to compare the basic parameters (V_b, S_b, statistical information) with different devices and discharge conditions is important for

finding the basic principle of blobs. In last year, we propose the PF scan (to change the pitch angle and connection length) and TF scan (to change the ECR layer position and thus main plasma position) experiments, which were done successfully to investigate blobs' characteristic in previous QUEST experimental campaign. Fast camera, radial probe and divertor probes are used to observe the blobs, as shown in Fig.4. In the new experiment during this visit, a new photron fast camera, with 70,000FPS, was used to observe blob size and velocity because the camera speed is higher than K-5(40,000FPS), which is used in last year. The shots, 25501# ~25511#, were done for observing blobs by Photron camera. Highly reproducible, current-free discharges of Hydrogen plasma are obtained by 2.45 GHz ECRH, with power P_{RF} ~ 10 kW. PF coil current is 1.1kA and TF coil current is 11kA. Typical plasma parameters, which is almost same with last year, in the edge of plasma are $n_e \sim 10^{16}$–10^{17} m^{-3} and $T_e \sim$ 1–12 eV, with peak values about as twice as higher than the background value. Other relevant parameters are $c_s \sim 10-34 km/s$, $\rho_s \equiv c_s / \omega_{ci} \sim 3-9 mm$. The new Photron camera data will be analyzed and combined with last year's data. The final result will be published in this year.

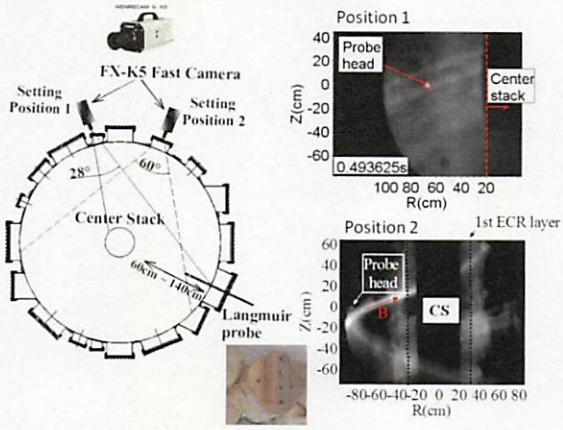

Fig. 4 (left)A schematic of combination of the Langmuir probe and the fast camera on QUEST for observing blob-filaments, (right) two typical images.

In this one week international joint research, progress on steady state operation (SSO) plasmas on QUEST and EAST was widely discussed, including the "Update on CFETR

Concept Design" and EAST 32s long pulse discharges. New blobs experiment in slab plasma on QUEST was fulfilled with new photron fast camera. Higher time resolution imagings were gotten and the data are under analysis now. The international joint study in EAST and QUEST would be energetic way on the SSO related issues in future.

Acknowledgement and comments:

Work supported by the international joint research at the Joint Usage of Research Centers for Applied Mechanics for 2013. We would like to thank our host, Professor K. Hanada, who helps a lot during my staying at QUEST and very appreciate the useful discussions and comments. We also give our thanks to Prof. Zushi, Prof. Nakamura, Assistant Prof. Hasegawa, Mr. Okina and Mr. Suzukawa, who gave us helpful discussions during our stay in Kyushu University. Our thanks are also expressed to the QUEST group.

It is a good chance for us to join in study in the QUEST. We hope that the international joint research at the Joint Usage of Research Centers for Applied Mechanics could continue to enhance China-Japan cooperation on fusion plasma research in the future.

(Signature) Xiang Gao, Haiqing Liu, Zhengxing Wang

(Name in print) Xiang Gao, Haiqing Liu, Zhengxing Wang

国際化推進共同研究概要

No. 4

タイトル: Develop and improve EFIT code of the plasma equilibrium reconstruction for SSO operation and advanced physical study on QUEST.

研究代表者: QIAN, jinping

所内世話人: 花田 和明

実 施 期 間: 2014 年 2 月 16 日 ～ 2 月 23 日

研究概要: QUEST に国際標準の平衡コード EFIT を導入して、平衡に関する検討を実施している。2月16日－23日の日程で来所し、IPN 配位を再構成するためにフラックスループの重みの最適化を行い、IPN 配位の再構成に成功した。
この結果の信頼性を確認するためにプラズマを上下に移動させて再構成した磁気面と2次元の軟 X 線計測との比較を行い、定性的一致することを確認した。

RESEARCH REPORT

Date Feb. 21 2014

Visiting scientist: (name) Jinping Qian

(position) Associate Professor

Visiting scientist: (name) Haiqing liu

(position) Associate Professor

Visiting scientist: (name) Zhengxing Wang

(position) Assistant Professor

Visiting scientist: (name) Xiang Gao

(position) Professor

(university / institute) Institute of Plasma Physics,
Chinese Academy of Sciences

Host scientist: (name) K. Hanada

(position) Professor

(university / institute) Kyushu University

Research period: (from) Feb. 16, 2014 (to) Feb.21, 2014

Research subject: **Equilibrium reconstruction on QUEST**

One aim of external magnetic measurements in tokamaks is to determine the shape of the plasma flux surfaces. To achieve this, many efficient methods and numerical codes for magnetic analysis have been developed. Among these, the fixed filament current approximation method seems to be the frequently used one. However, preset plasma current filament locations should be assumed in this method while the plasma position is unknown. Moreover, the method is not to solve the MHD equilibrium equation. This will affect the accuracy of the plasma shape reconstruction. Another method parameterizes the unknown current profile with a suitable set of test functions. An iterative process is also used in this procedure. One of the most widely used is EFIT code.

In an axisymmetric toroidal system, the MHD equilibrium Grad-Shafranov equation can be written as

$$\Delta^* \psi = -\mu_0 R J_\phi \quad , \qquad J_\phi = RP'(\psi) + \frac{\mu_0 FF'(\psi)}{4\pi^2 R}$$

Here, ψ is the poloidal magnetic flux per radian of the toroidal angle ϕ enclosed by a magnetic surface, $F = 2\pi R B_\phi / \mu_0$ and B_ϕ are the poloidal current function and the toroidal magnetic field, and $\Delta^* = R^2 \nabla \cdot \left(\nabla / R^2 \right)$. The toroidal plasma current is defined by the two flux functions P' and FF', which are the plasma pressure gradient and the poloidal current function, respectively. In general, the two flux functions are arbitrary with a set of free parameters. A general set of polynomial basis functions is chosen of the form

$$P'(\psi) = \sum \alpha_n y_n(x)$$

$$FF'(\psi) = \sum \gamma_n y_n(x),$$

where $x = (\psi - \psi_0)/(\psi_1 - \psi_0)$ is the normalized poloidal magnetic flux, ψ_0 and ψ_1

are the poloidal magnetic flux at the magnetic axis and at the plasma boundary, and $0 \le x \le 1$.

The Quest (Q –shu University Experiment with Steady State Spherical Tokamak) project focuses on the steady state operation. Phase I (in these two years) in the project is to make full current drive plasma up to 20kA and it is running from Otc. 2008. Closed divertor will be desighed and tested in the Phase II. The magnetic measurements consist of 67 flux loops, 1 Rogowski loop (see Figure 1). The equilibrium configuration is also shown in figure 2 based on QUEST designed parameters.

A very important part of the equilibrium reconstruction is the benchmarking of the external coil inductions against experimental measurements and the testing of the adequacy of the magnetic diagnostic data used for the equilibrium reconstruction. The benchmarking was performed in 2010 and further discussions of uncertainty are done with Prof. Zushi during the visit.

The validation of EFIT proposal is performed by the pre-program control the HCUL coil current with the horizontal field to push the plasma up and down (shot 25477-25479). Meanwhile, the 2D SXR camera is mounted for the double checking of the equilibrium reconstruction of EFIT. To study the property of the edge turbulence on QUEST, the superfast camera is used to observe the Blob phenomena. During the visist, Prof. Gao gave a presentation of CFETR concept and design.

In this part, the reconstruction examples using external magnetic data are presented to illustrate equilibrium reconstructions on QUEST (fig2-4). The reconstructions are done using the polynomial representation for P' and FF'. A 65×65 (65 grid points in the R and Z direction) version of EFIT is used with a relative equilibrium convergence error (10^{-3}). Figure 5 overlays the reconstructed Z position and the horizontal coil HCUL. When the HCUL current cut to zero, the plasma goes back quickly at 7.5s. The roughly analysis of 2D SXR emissivity matches the Z perturbation. More analysis should be done to further confirm the EFIT equilibrium reconstruction activities.

In all, the off-line EFIT reconstruction has been successfully performed on QUEST

device. This will be helpful for further physical study and the steady state operation

Acknowledgement:

We would like to thank our host, Professor K. Hanada, who helps a lot during our staying at QUEST and very appreciate the useful discussion and comments.

Figure captions:

Figure 1 Quest device cross-section with flux loops (open circle)
Figure 2 Medial Z position reconstruction (shot25477)
Figure 3 Minus Z position reconstruction (shot25478)
Figure 4 Positive Z position reconstruction (shot25479)
Figure 5 Overlays of equilibrium Z positions (shot 25477-25479)

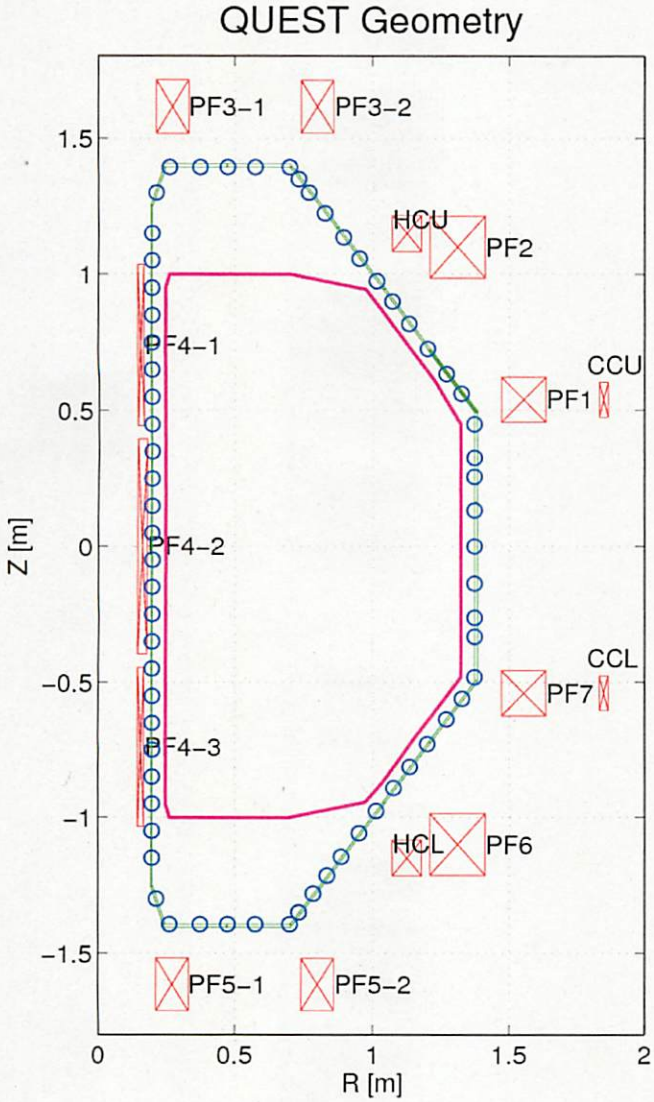

Figure 1 Quest device cross-section with flux loops (open circle)

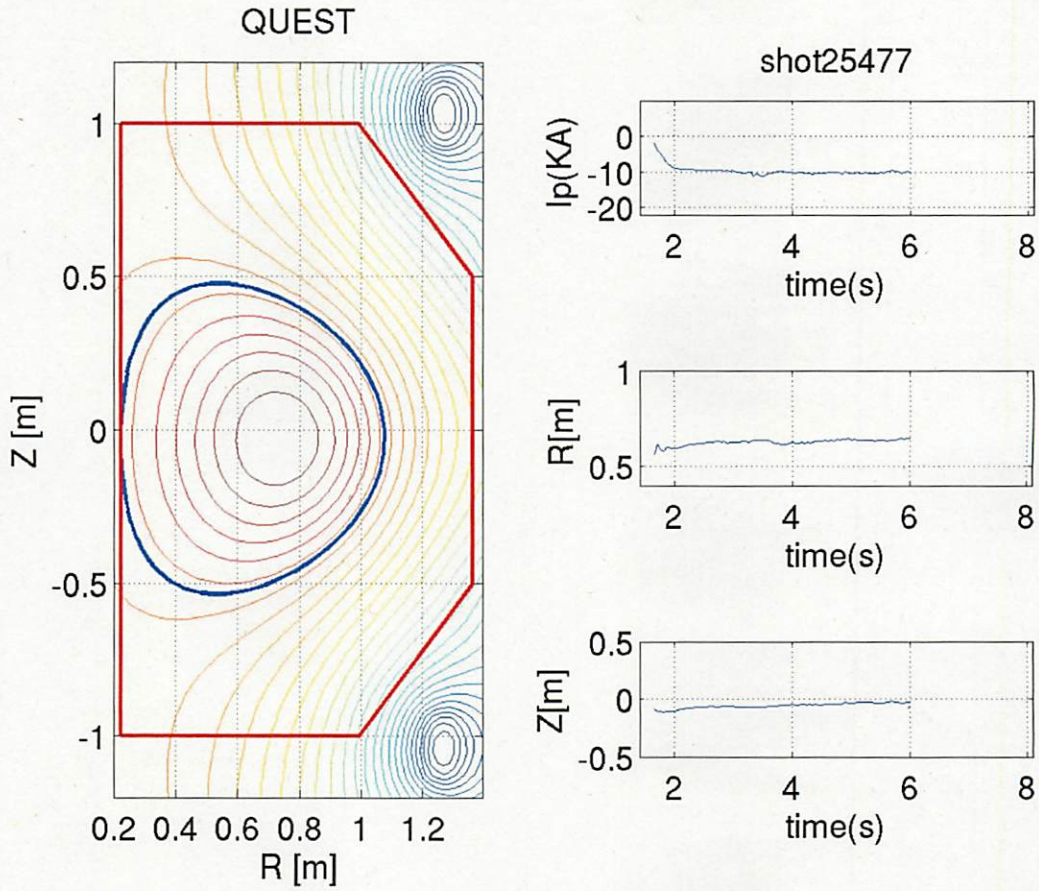

Figure 2 Mid Z position reconstruction (shot25477)

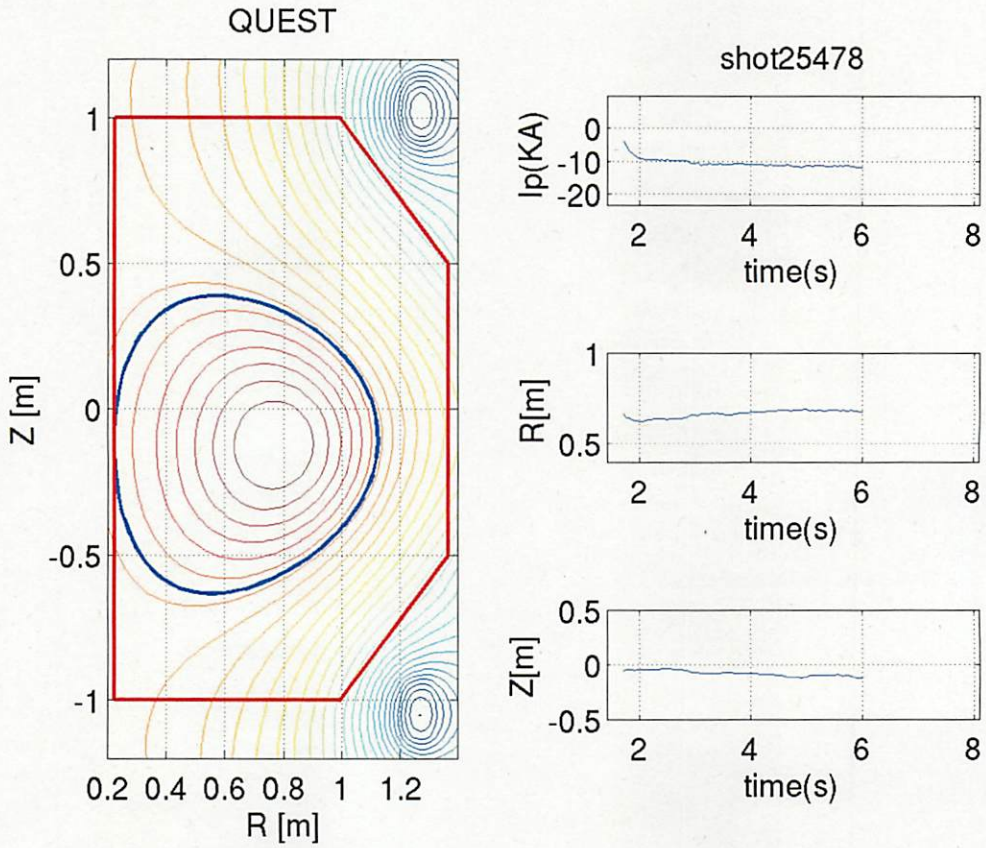

Figure 3 Minus Z position reconstruction (shot25478)

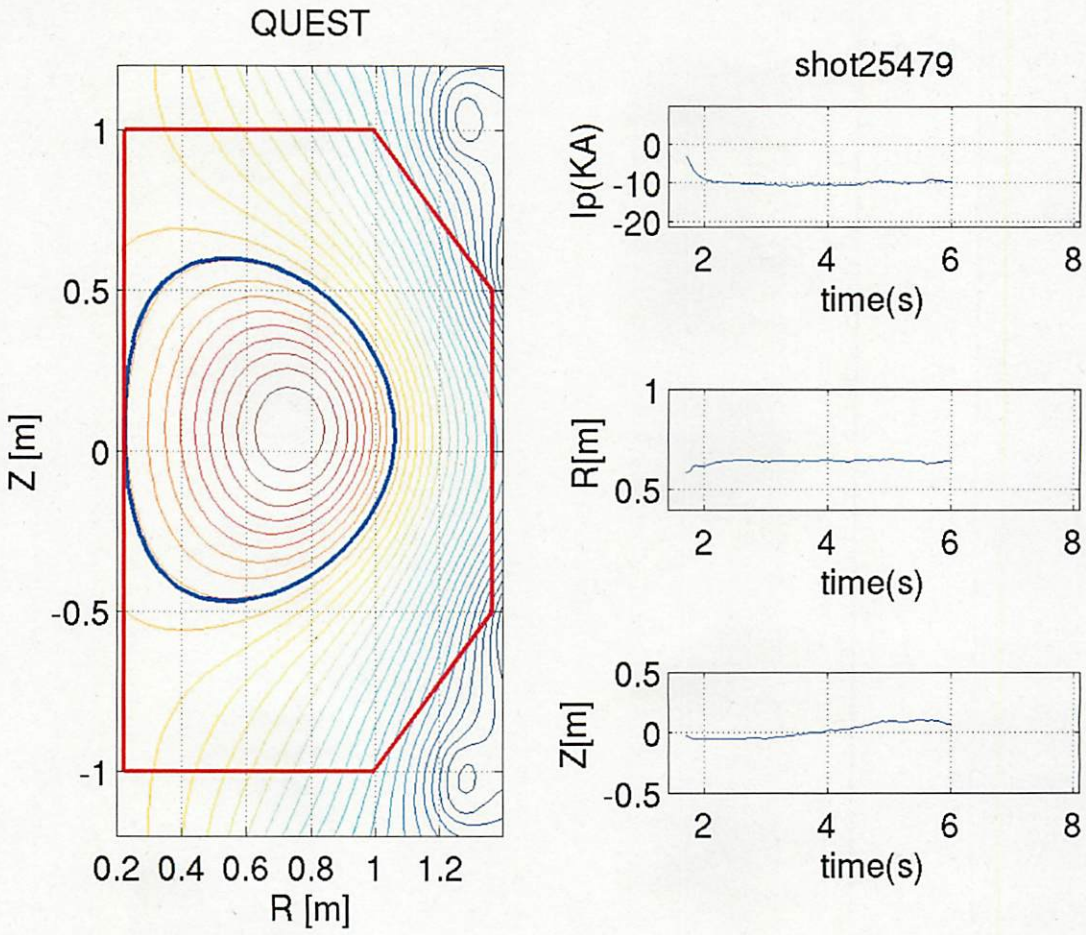

Figure 4 Positive Z position reconstruction (shot25479)

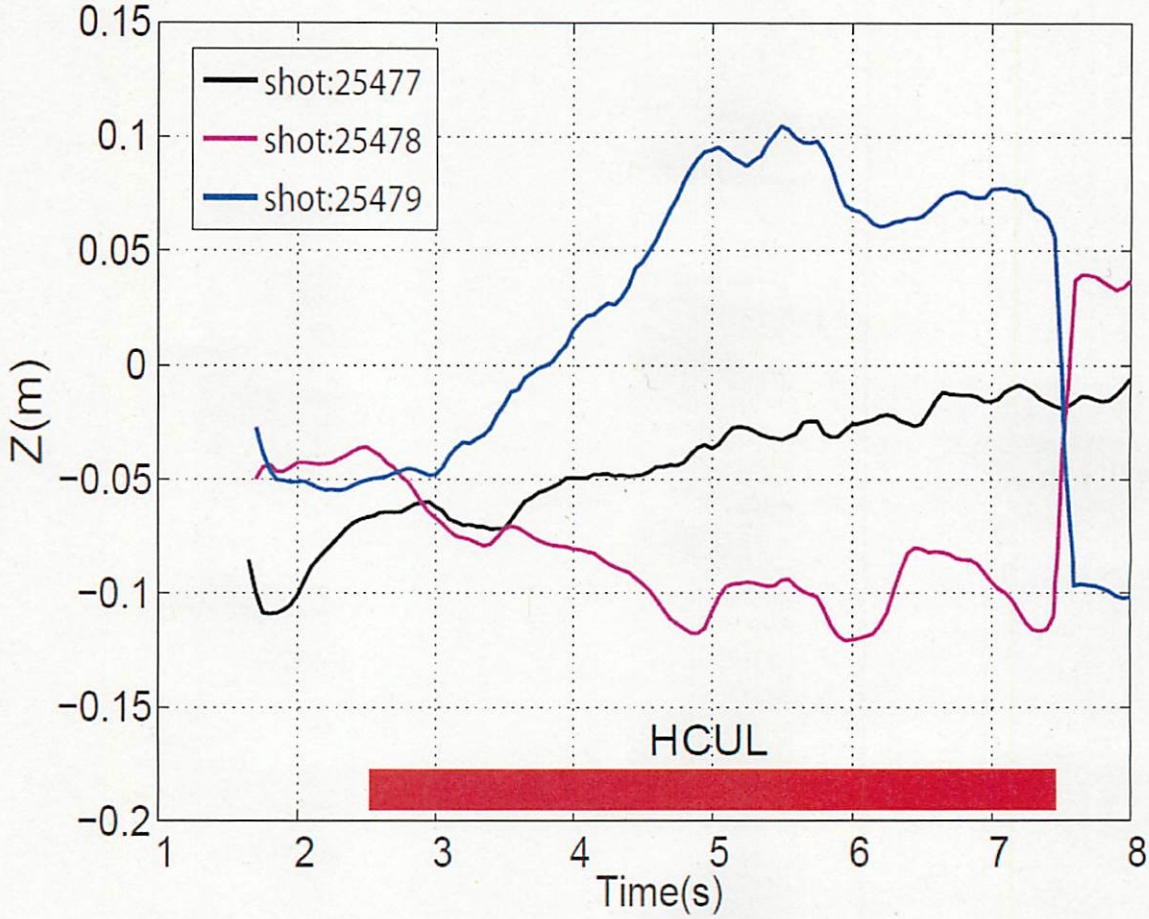

Figure 5 Overlays of equilibrium Z positions (shot 25477-25479)

(Signature) J. Qian

(Name in print) Jinping Qian

国際化推進共同研究概要

No. 5

タイトル: Collaborative research on QUEST-EBW current drive with divertor, wall and recycling control.

研究代表者: PENG, Yueng-Kay, Martin

所内世話人: 花田 和明

実 施 期 間: 2014 年 2 月 24 日 ～ 2 月 26 日

研 究 概 要:2月24日～26日の日程でWSが開催された。参加者は、外国人4名(TV meeting 1名を含む)、学外者4名、学内者8名であり、球状トカマクの最大の課題であるプラズマの非誘導電流駆動による立ち上げについて議論を行った。昨年度の会議で電子流体とイオン流体を個別に扱う平衡に関して議論が進み、今年度には共著で論文を作成した。今年度はQUESTで得られているプラズマの回転の観測や2nd ECCDについての議論が行われた。

Report of 2nd workshop on QUEST and related ST RF startup and sustainment research

Kyushu University, February 24 – 26, 2014

Participants

A. Ejiri, The University of Tokyo

K. Hanada (Co-Chair), Kyushu University

T. Fujita, Nagoya University

Z. Gao, Tsinghua University, P.R.C.

H. Idei, Kyushu University

A. Ishida, Niigata University

T. Maekawa, Kyoto University

M. Peng (Co-Chair), The University of Tokyo

R. Raman, University of Washington, U.S.A.

Y. Takase, The University of Tokyo

H. Zushi, Kyushu University

V. Shevchenko, Culham Center for Fusion Energy, U.K.

Introduction (M. Peng)

A workshop dedicated to the subject of radiofrequency (RF) startup and sustainment plasma research on QUEST and related spherical tokamak (ST) experiments in Japan and U.K., was held at the Research Institute of Applied Mechanics (RIAM), Kyushu University during February 26 – March 1, 2013. The workshop was attended by 20 research leaders, researchers, and graduate students, from Kyushu University, the University of Tokyo, Kyoto University, National Institute for Fusion Science, Niigata University, Oak Ridge National Laboratory (ORNL, U.S.A.), and Culham Center for Fusion Energy (CCFE, U.K.).

RF plasma startup and sustainment, including sustained plasma-wall interactions, is a remaining research gap to be filled to realize compact, cost-reduced ST fusion energy applications.

Eighteen presentations were made and were accompanied with extensive discussions. The participants obtained substantive common understanding of the key scientific and technical research issues of interest, and developed recommendations of the next research steps to take to resolve these issues.

The following summarized the results of this workshop, organized as follows:

Overall workshop summary

1) Solenoid-free RF-only ST and tokamak plasmas, and current hole plasma properties (T. Maekawa)
2) RF technology and diagnostics (Y. Takase)
3) Two-fluid multi-component plasma equilibrium modeling for RF-only ST plasmas, including possibility for current hole tokamak plasmas (M. Peng)
4) Long-pulse heat and particle handling (K. Hanada)
5) ST designs for hot wall and CHI on QUEST (K. Hanada)
6) Research and collaboration suggestions for JFY 2014 (M. Peng)

1) Solenoid-free RF-only ST and tokamak plasmas, and current hole plasma properties (T. Maekawa)

Solenoid-free RF-only ST and tokamak plasmas using various waves, including ECW/EBW, LHW and AW, have been investigated and/or generated on various devices from small to large devices of STs and Tokamaks worldwide. Most of experiments have been done using ECW/EBW. In particular, most recent experiments using 28 GHz gyrotrons on QUEST and MAST was able to start up the current up to Ip= 66 kA and 73

kA, using 270 kW and 60 kW of powers, respectively. While their ECH schemes are quite different each other; 2nd harmonic X wave ECCD on QUEST and EBWCD at fundamental EC resonance on MAST, their quite low density operation at ne=0.1-0.5 $x10^{-18}m^{-3}$(~0.01-0.05 of the cutoff density) seems to bring above results, providing new schemes to be investigated toward completion of RF startup. In addition interesting is found to be the current hole in which similar issues as in RF-only plasmas in equilibrium and stability characteristics remain unresolved.

On QUEST plasma currents up to 66kA have been non-inductively started up by injecting 28GHz 270kW power for second harmonic resonance EC heating. The power was launched perpendicularly to the toroidal field in the form of X-mode from an open cut of corrugated circular waveguide (carrying HE11 mode) on the mid-plane. The electron density was as low as $0.3\sim0.5x10^{-18}m^{-3}$ and the current was carried by energetic electron tail. The radiation lobe is estimated to have a significant fraction of power around N//~-0.5 at the resonance layer, which may drive the tail electrons via Doppler shifted EC resonance in front of the cold 2nd harmonic resonance layer at R=0.32 m. The 2nd harmonic EC heating of bulk electrons was also clearly shown on Te profile on mid plane. While the highest current of 66 kA was obtained with a slow ramp of Bv, A 54 kA of plasma current was sustained for 0.9 sec under a steady Bv at the linen averaged density of $0.5x10^{-18}m^{-3}$. Recharging of CS was also obtained by injecting RF into an ohmically initiated target plasma under feedback regulation of Center Solenoid (CS) coil current to keep plasma current constant. Attempts have been made to conduct EBW current drive experiments by injecting 8.2 GHz power into target plasmas maintained by 28 GHz 2nd harmonic EC heating.

Experiments on JT-60U, DIII-D and KSTAR suggest that initial small closed flux surface can be produced solely by ECH. In particular recent experiment on KSTAR suggests that the current inside the last closed flux surface was already driven by ECCD. In the experiments of JT-60U and KSTAR, however, just after the formation of initial small closed flux surface the current began to terminate with a flash on the vessel wall that suggests strong hitting of EC-heated electrons. There appeared a large mirror-confined area around the small closed flux surface. The energy range of the mirror-confined tail electrons increases as the product of R and Bv increases, suggesting that the hitting problem becomes serious in large-major-radius tori. These results imply that some appropriate methods are needed to avoid strong interaction of energetic electrons with the vessel wall upon the appearance of an initial small closed flux surface

to expand the surface to a large solid closed flux surface to confine a high temperature plasma. If a high temperature and low resistivity plasma could be non-inductively started up by ECH/ECCD, no resistive cut would be needed for the core structure to ensure getting through of OH high loop voltage for the initial current startup, which is beneficial for reactors.

On JT-60U RF preionization, controlled I_p ramp-up by B_v ramp and RFCD, and transition to NB heated advanced tokamak plasma (ITB + H-mode $\beta_p = 3.6$, $\beta_N = 1.6$, $H_H = 1.6$, $f_{BS} > 90\%$) was demonstrated. BS-sustained plasma was obtained by only counter and perpendicular NBI. Such a plasma exhibits repetitive β collapse (by kink-ballooning mode) and a gradual deterioration of ITB. Addition of co NBCD was helpful for achieving steady sustainment of I_p. Evidences of BS overdrive ($V_l < 0$ and CS recharging, or I_p ramp-up with $V_l = 0$) were observed. Extension of these results to higher I_p and a more complete characterization of controllability of such a plasma remain topics of further research.

On TST-2 ST plasma initiation and I_p ramp-up by waves in the LH frequency range were demonstrated using three types antennas: inductively-coupled combline (ICC) antenna, dielectric-loaded waveguide array (grill) antenna, and capacitively-coupled combline (CCC) antenna. Spontaneous formation of ST configuration with closed flux surfaces was observed. At low I_p (< 2 kA), I_p is dominantly pressure-driven, and is independent of the wave type. At higher I_p (> 5 kA), I_p becomes mainly wave-driven, and control of the j profile by externally excited waves should become possible. Highest η_{CD} was realized by the CCC antenna at high n_e

On MAST non-solenoid EBW assisted plasma start-up has been demonstrated using a long pulse O-mode injection. Injected RF power was about 60 kW as measured close to the vacuum window. RF pulse was varied in duration up to 440 ms. Maximum plasma current achieved was about 73 kA which is more than twice higher than a previously obtained value of 33 kA. To our knowledge this is the highest value observed so far in the EBW start-up experiments. The current drive efficiency (CDE) achieved in these experiments was higher than 1A/W. Such high values were previously obtained only with lower hybrid CD. The main result of these experiments is the linear rise of plasma current during RF injection. This fact suggests that actual CDE is higher than current dissipation processes at present RF power levels and the range of RF pulse duration. So the actual CDE must of the order of 3A/W. Thus according to estimates based upon

current decay time measurements, plasma current is expected to rise further for about 1 sec with the extended pulse length at 60 kW of RF power. That means plasma currents over 200 kA are achievable with only 60 kW 1.5 sec pulse.
It was found experimentally that RF driven current in MAST is linearly dependent on RF power injected within the power range from 25 kW to 50 kW. If such linear dependence is extrapolated towards higher RF power then potentially currents up to 700 kA could be achieved in MAST with 200 kW available from the ORNL gyrotron.
It was confirmed that plasma current is carried predominantly by supra-thermal electrons with the energy of 100 keV. No relativistic electrons were observed during initial plasma formation as well as during a current ramp-up phase. This conclusion is based on multi-angle EC emission observation during all phases of EBW start-up scenario.
Experiments with vertical modulation of the plasma magnetic axis have been conducted to validate RF current drive mechanism. Plasma current showed an anti-phase response to the vertical modulation which suggests that plasma current was predominantly driven by EBWs.

SUNIST has conducted RF startup using ECW/EBW and AWCD. In the case of ECW/EBW startup a plasma current of about 2 kA was obtained with a steadily applied vertical field of 12 Gauss and 40 kW microwave injection in the SUNIST. Especially, the transient process at the very beginning of the startup was both experimentally studied and simulated. A new 5 GHz microwave is being built, whose duration will be more than 50ms and then be able to be employed to study the current ramp-up by ECW/EBW mode conversion. Related to experimental efforts, theoretical studies are performed as well. The LFS injected ECW experiences the O-X-B conversion to become the EBW. The window for O-X conversion is narrow and sensitive for parameters of plasma, wave and field and, also, the X-B is not hundred percentages. Therefore, the conversion efficiency should be paid more attention in EBW experiments, especially in future application with high power injection.
AWCD has a potential high efficiency, but may dramatically decrease due to electron trapping. The scheme of so-called non-resonant current drive or helicity injection current drive in the steady status is over-estimated at least, a spatial redistribution of parallel force within resonant mechanism for AW needs specific arrangement. Neoclassical effect may recover some of efficiency, but it depends on the long-time behaviors, for example the competition between flow drive and current drive. Experimental efforts should be made to verify/ clear up the time scales in concerning

different behaviors for AWCD.
Experimental plan of AWCD is ongoing in the SUNIST. Preliminary experimental results have been obtained with 60 kW / 0.6~0.9 MHz rf power and two pairs of unshielded antennas. The increases of impurities and antenna impedances are found. It is also found that the low phase velocity waves have some effects on accelerating runaway electrons. At present, the Alfven wave antenna system was equipped with BN limiters, which is expected to improve the wave coupling. Also, a new low frequency rf source was equipped on the SUNIST, which can control the phases of four outputs. Improved experiments are expected.

The current hole (CH) is a region with nearly zero poloidal field observed at the center of tokamak plasma. The current hole is characterized by very small B_p inside, but how small it is is not well identified, with present accuracy of B_p measurement, to address some physical issues including equilibrium and particle (electron) orbits. Some models of the magnetic field structure (MHD equilibrium) of current hole plasma are proposed. Dynamics of current hole plasma was studied, including nonlinear MHD simulations. However, no conclusive picture on the MHD equilibrium has been identified. Current induced by fast particles are calculated, but no equilibrium analysis consistent with it has been made. Such analysis would be commonly used for CH plasmas and for RF-only STs. In the discussion, it was pointed out that centrifugal force due to finite toroidal rotation inside the current hole should be included in the equilibrium analysis.

2) <u>RF technology and diagnostics (Y. Takase)</u>

A 28 GHz system was developed under collaboration among Kyushu University, University of Tsukuba, and NIFS, and was used to generate RF produced plasmas with Ip > 50 kA on QUEST. In 2011, an anode power supply system, a gyrotron tank, and associated equipments were prepared at Kyushu University to operate Tsukuba's 28 GHz gyrotron. In 2012, all gyrotron and transmission line components were installed and adjusted. In 2013, ECH/ECCD experiments were conducted using the 28 GHz system.
Polarization control of the injected EM wave to optimize coupling to the EB wave in LATE was shown to be effective for generating and sustaining highly over-dense plasmas.
RF launchers to excite a uni-directional traveling wave were developed for the TST-2

lower hybrid current (LH) drive experiment. Four-waveguide dielectric-loaded waveguide array was used to study the dependence of LH current drive on the excited wavenumber spectrum. A capacitively-coupled combline (CCC) antenna was developed to achieve better directionality and sharper wavenumber spectrum. The highest current drive efficiency was obtained using the CCC antenna.

Various diagnostics have been developed to study the physics of plasmas generated and maintained by only RF power in TST-2. Optics with adjustable angular orientation of the sightline have been installed on the visible spectrometer system to measure the flow velocity and the temperature of impurity ions. CIII (C2+) line emission from LHW sustained plasmas (with Ip ~ 6.4 kA) was measured. The measured flow velocity in the toroidal direction was small (< 1 km/s). The flow velocity in the poloidal direction was larger (~ 3 km/s), and indicated the presence of a positive radial electric field (~ 200 V/m). Measurements of OH plasmas using a double-pass Thomson scattering system revealed an anisotropic temperature due to the inductive toroidal electric field. A multi-pass Thomson scattering system has been developed and a round-trip efficiency of 70-75 % was demonstrated. Further improvements are required to measure RF generated plasmas with very low density. Local current density in the edge region of an OH plasma was measured by a Rogowski probe. Further improvements are being implemented to measure RF generated plasmas. Wave polarization and wavenumber have been measured with newly developed electromagnetic and electrostatic RF probes.

A heavy ion beam probe (HIBP) system has been installed on LATE. Quadrupole lenses have increased the beam current at the energy analyzer. By controlling the Rb ion beam orbit, secondary beam current from the ST plasma (Ip ~ 7 kA) maintained solely by EBW was detected for the first time. Preliminary results indicated that the space potential φ near the ECR layer near the midplane is -20 ~ -30 V. Improvements are required to measure the potential profile over the whole cross section inside the LCFS. A further focusing of the initial ion beam should be realized to reduce the beam divergence, and better target plasmas with higher density and higher electron temperature should be developed to obtain sufficient secondary ionization events of the probe ion beam.

3) Two-fluid multi-component plasma equilibrium modeling for RF-only ST plasmas, including possibility for current hole tokamak plasmas (M. Peng, A. Ishida)

The RF-startup and sustained ST plasma experiments such as TST-2, LATE and QUEST indicate
that electron temperature is much larger than ion temperature and significant toroidal current density flows outside the last closed flux surface (LCFS). After the first workshop held at Kyusyu University (February 26 - March 1, 2013) we have applied our two-fluid axisymmetric equilibrium model [1, 2] to reconstruct these equilibria [3]. In so doing, it has been recognized that the two-fluid model is not satisfactory to describe such plasmas. Therefore, in this second workshop we presented mainly the formulation of the four-component axisymmetric equilibrium model. This model contains twelve profile functions that are represented by arbitrary functions of species generalized angular momentum. We are developing a code for numerical computation. We hope we will be able to show some results of this more complex model in the next workshop. Even though using more approximate three-component model it is demonstrated that low-density, high-temperature electrons which are driven directly by RF carry significant current and extend even in the open field region while relatively high-density and low-temperature ions and electrons carry less significant current and localized within the last closed flux surface.

[1] A. Ishida, L.C. Steinhauer, Y.K.M. Peng, Phys. Plasmas 17, 122507 (2010).
[2] A. Ishida, L.C. Steinhauer, Phys. Plasma 19, 102512 (2012).
[3] Y.-K.M. Peng, A. Ishida, et al., accepted for publication in PFRJ (February, 2014)

4) Long-pulse heat and particle handling (K. Hanada)

Power balance was completely obtained by cooling-down of plasma facing components (PFCs) even in long duration discharges more than 300s on QUEST. Particle balance is still under investigation and progression from low (LR) to high recycling (HR) was observed in long duration discharges on QUEST. Several thermal desorption spectrum (TDS) was obtained with plasma-exposed specimen and their feature can be reconstructed on the basis of a model calculation. The calculation gives an interpretation that the applied hydrogen fluence is possible to give a saturation in the recycling ratio, R_{rec}, of unity around the progression from LR to HR.

5) ST designs for hot wall and CHI on QUEST (K. Hanada)

Design activities for a CHI system and a hot wall were introduced in the WS. The CHI system will be installed in this summer and it has the possibility to make a 150 kA plasma current on QUEST. An electrode should be located at lower than present divertor plate by 30cm and charge up with a capacitor bank via an isolated cable.

After making discharge between the electrode and a hot wall, plasma will expand with a j x B force in the whole of the QUEST vessel. And then the plasma will heat up with ECH, and consequently a high current and temperature plasma will be achieved.

A hot wall will be also installed in this summer and has the capability to keep a wall temperature at 300-500 centigrade even during plasma discharges. The hot wall has a heating and a cooling systems and especially the cooling system has two kinds of water-cooling channel with different thermal resistance to avoid overmuch cooling.

6) Research and collaboration suggestions for JFY 2014 (M. Peng)

1) The polarizer for B-mode injection of 2.45GHz has been developed in LATE, and a 2.45GHz, 50kW system is running for ECR cleaning on QUEST. These two components is likely to match and may make a good combination to investigate a scaling in different size of machines.
2) Installation of a polarized mirror for 28GHz on QUEST is a candidate to do an EBWCD experiments, which seems to be promising in MAST. In the QUEST project, it is important to make a higher density plasma and EBWCD is the most efficient tool to do it.
3) Transient CHI experiments will start in 2014 A/W experimental campaign. This is a promising way to make plasma start-up and a 28GHz ECH will give a good combination to heat plasma. Consequently a higher density and current plasma will be obtained.

国際化推進共同研究概要

No. 6

タイトル：Feasibility study for solenoid-less plasma start-up capability in quest using transient coaxial helicity injection.

研究代表者： RAMAN, Roger

所内世話人： 花田　和明

来訪期間 ： 2014 年 2 月 24 日 ～ 3 月 5 日

概要： 2月24－3月5日の日程で来所した。昨年度まで概念設計を行っていた同軸ヘリシティ入射(CHI)を QUEST で実施するための予算が米国で認められたため、来年度の CHI 設置に向けて詳細設計を行った。CHI は来年度夏に QUEST に設置されて実験が開始される予定である。

Implementation of CHI on QUEST
28 February 2014

R. Raman[1], T.R. Jarboe[1], M. Ono[2], K. Hanada[3], et al.,
[1] University of Washington, Seattle, WA, USA
[2] Princeton Plasma Physics Laboratory, Princeton, NJ, USA
[3] Kyushu University, Kyushu, Japan

During the past year the details for implementing Coaxial Helicity Injection (CHI) capability on QUEST were finalized. In this report we summarize the final configuration of CHI on QUEST. This report is an update to the previous report dated 29 January 2013. Therefore, information from the previous report is only mentioned briefly, so as to make this report easier to read.

On QUEST, CHI is capable of playing multiple roles. These include: (1) Solenoid-free plasma start-up: CHI can generate significant amounts of plasma current through the process of *transient* CHI. (2) Edge biasing: By driving few kA of current along the outer scrape-off-layer (SOL), it provides a means to inject or deplete density along the SOL and thereby modify the edge density and vary the density gradient near the separatrix region in support of EBW current drive studies. (3) Steady-state current drive: By continuously driving current along the scrape-off-layer, it offers the possibility of continuous current drive to modify the edge current profile. The SS CHI approach can also be applied in a pulsed mode to provide current feedback control. The all metal nature of QUEST in addition to its capability for high ECH power should both reduce the amount of low-Z impurities initially injected during the application of CHI and because of its ECH heating capability allow a relatively greater fraction of the injected low-Z impurities to burn through radiation barriers, which is necessary for a good confinement discharge.

CHI Electrode Configuration after 2012 activities:

Figure 1 shows the configuration of the CHI electrodes after the conclusion of the previous year's activities. The main aspects of the design are as follows:

- A 42 cm wide electrode is mounted on top a 27 cm wide baseplate. These are bolted together at many locations, such that one base plate connects to two electrodes and an electrode is connected to two base plates in an interleaving manner. Thus, after assembly this becomes a continuous single structure.
- These were mounted on top a 42 cm wide insulator that was 2 cm thick.
- The insulator, and the assembled metallic plates are mounted on top of the existing divertor, which is lowered from its original location by 13 cm.
- The lower divertor plate, insulator plate, and the electrode assembly are all connected together using ceramic bolts.
- Current is fed from three toroidal locations using 2.5 cm diameter stainless steel rods.

- The Alumina and electrode plates are mounted on the QUEST divertor plate, which is lowered by about 13 cm. This requires reducing the height of the divertor plate support legs by 13 cm.
- Electrical isolation is achieved between the current feed rod and the QUEST vessel using a ceramic current feed through and a bellows arrangement.

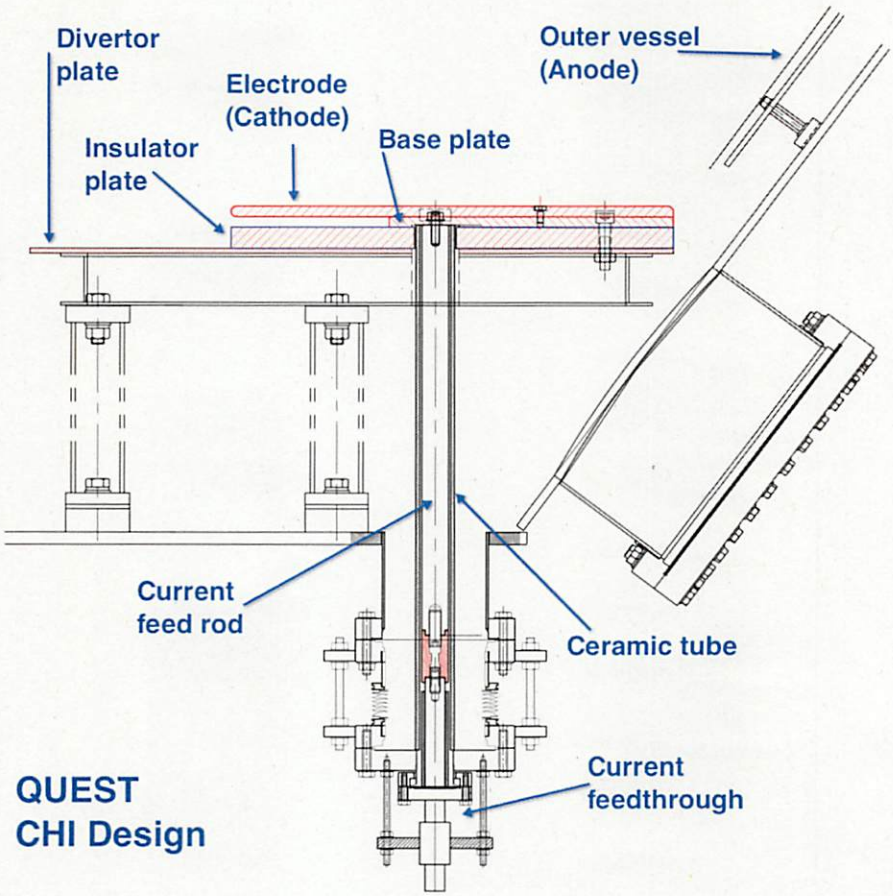

Figure 1: The figure shows the location of the electrode assembly on top of the divertor plate. Gas would be injected in the gap between the outer edge of the electrode plate and the outer vessel structure. The gas injection ports would be located on the same ports that contain the cryo pumps. The injector current is fed through the current feed rods that are designed to handle the J x B forces resulting from the interaction of the injector current with the external toroidal field.

Improvements to the CHI Electrode Configuration:

Much of the changes that were made to the design were to simplify it, and to increase the strength of some components. The configuration is also revised to make it compatible with the QUEST 'hot-wall' components. The company that is responsible for detailed design of the CHI components is now in the process of generating the final design drawings. So, the changes made to the previous configuration are described briefly. Later

during 2014, an update to this report will be provided that includes the actual design drawings.

Electrode and baseplate connections: These remain the same as before, and form a continuous single structure. This is referred to as the electrode assembly.

Electrode assembly connections to the insulator plate and the divertor plate: The ceramic bolts connecting these together have been removed. Instead a 2 mm lip is added to the insulator plate in the region not covered by the base plate. This constrains the insulator plate from moving radially out. The insulator plate, and the electrode assembly are fixed in place by the three current feed rods at three toroidal locations. As before, the lower (non-plasma facing side) of the electrode plate would be coated with a ceramic insulator.

Insulator plate: As noted above, the thickness of the insulator plate in the region not covered by the base plate is increased from 20 mm to 22 mm. in addition, of the 8 plates required for the insulator, 7 would be identical and the final 8^{th} plate would have symmetrical lips at the edges so that it could be installed from the top – instead of sliding it from the edge.

Ceramic bolt holes: The ceramic bolt holes that were present on the insulator plate, divertor plate, base plate and electrode plate have all been removed.

Current feed assembly: This has been considerably simplified and strengthened. A concern with the previous design was that, even after sufficiently strengthening all components, there is still a possibility that the interface between the ceramic and the conductor within the commercially purchased ceramic break could fracture. The arrangement was also quite complex. The revised version has the following changes.

- The stainless steel rod diameter will be increased from 2.5 cm to up to 4 cm.
- The corresponding diameter of the ceramic tube that surrounds the SS tube will be increased to the extent possible, as this may be determined by commercially available tube sizes. This also determines the maximum diameter of the SS rod.
- The SS rod will continue to be connected to the base plate using M8 bolts.
- The SS rod length will be increased sufficiently to permit other modifications described below.
- The current feed through, as well as the connector between the SS rod and the current feed rod is eliminated. Instead, a cylindrical Vespel insulator that makes a dual O-ring seal on the surface of the SS rod replaces this. On the outer diameter of the Vespel insulator it makes dual O-ring seal with the inner wall of a stainless steel cylinder. The cylinder has two flanges. The top flange is connected to the QUEST vessel port to be used for the current feed rod. An interface plate between the two flanges would provide some flexibility to compensate for the variations in the exact location of the SS rod.
- The lower flange would be connected to a circular current feed plate that will be connected to the center conductor of up to 10 RG214 coaxial cables. The current feed plate would be fabricated out of copper.

- The Vespel insulator dimensions would be adjusted to ensure that the electrical tracking length along its surface is at least 5 cm.
- A locking ring (below the Vespel) that clamps on to the SS rod will be used to ensure that the gap between the ceramic rod and the Vespel is minimized.
- A second circular current feed plate would be attached to the SS rod and located below the locking ring. This would be fabricated out of copper.
- 2 cm long copper tubes of ID about 7.5 mm would be brazed on to the copper plate, and distributed uniformly, and toroidally around the plate. This would be used to make connections with outer braid of RG214 coax cables.

Gas injection: At three toroidal locations, gas injection assemblies would be installed. These would be made of 5 cm diameter SS tube bent to approximately conform to the circular radius of the QUEST vessel at the installation location. It would be approximately 35 to 40 cm in length. Each of these assemblies would have 5 holes drilled in them that vary from 1 cm in diameter for the central port and 3 cm in diameter for the port farthest from the center.

Hot-Wall shield: The present design of the lower hot-wall on QUEST results in a large opening between the vessel wall and the inner wall of the hot-wall components. This would have the effect of channeling some of the CHI discharge into this region behind the hot-wall and the vessel. To avoid this, a toroidal metallic skirt would be added that extends from the lower edge of the hot wall to the vessel wall. In addition to covering the open gap, this would provide a more desirable anode surface for the CHI discharge.

Initial operating configuration:
The plasma-facing surface of the electrode may not be coated with tungsten for the initial operations in 2014. A refractory material surface will be added to this component after the initial CHI experiments. The plasma-facing surface of the hot-wall skirt may also not be coated with refractory material for the first CHI discharges.

US Hardware Contributions:

The US would provide the following components.

- Primary insulator
- Ceramic discs to cover the holes in the ceramic insulator not required for the current feed rod
- Coax cables and banana plugs to interface to the current feed plates
- Gas injection system that connects to ports on the QUEST vessel, where the gas injection assemblies are installed
- Capacitor bank to power CHI
- Control system to operate the capacitor bank and the gas injection system

国際化推進共同研究概要

No.7

タイトル：Thermal emission measurements with phased array technipue.

研究代表者：SHEVCHENKO, Vladimir

所内世話人： 出射 浩

来訪期間： 2014 年 2 月 24 日 ～ 2 月 26 日

概要： 2月24日～26日午前までに開催されたWS に参加し、QUEST での 2ndECCD 等について議論した。26日午後、27日は、位相配列・アダプティブアレイアンテナによる熱輻射計計測について議論された。双方からアンテナ低電力試験結果、位相配列・アダプティブアレイによる観測結果が示され、問題点の洗い出し、解決へのアプローチが議論された。併せて位相配列・アダプティブアレイを用いた反射計計測についても議論された。

Thermal emission measurements with phased array technique

CCFE, Culham Science Centre, UK ,Vladimir Shevchenko

Statement of goals and objectives:

The objective of this bidirectional research is aimed at developing a microwave imaging technique using remote sensing array antenna to measure electron cyclotron/Bernstein emission (ECE/EBE) from high temperature plasma confined in toroidal geometry. In QUEST project at Japan , such measurement is being developed using phased waveguide array antenna and at MAST project at UK, special Vivaldi antenna is employed using synthetic aperture imaging technique. The present collaboration is helpful in strengthening our understanding and sharing common problems and issues regarding such diagnostics.

Diagnostic objectives:

The mode converted Electron Bernstein Wave (EBW) heating and current drive is one of the most attractive choice for steady state operation of spherical tokamaks. In QUEST, O-X-B mode conversion scenario is employed [1], where efficient mode conversion is critically dependent on the optimal launch angle of O-mode wave launched to its cut-off layer and the density gradient present there. The optimum injection angle of the heating wave can be determined by finding the viewing angle that maximizes the thermal emission intensity in the over dense plasma. This can be done through the radiometric measurements of these emissions. The thermal emission measurement will be useful to study plasma turbulence and temperature fluctuation. Additionally, this can be envisaged for active interlock of high power auxiliary system in future fusion reactors.

Diagnostic details:

In QUEST it is envisaged to develop emission measurement technique with the help of standard phase array waveguide antenna used for EC or Lower Hybrid systems in tokamaks without using any active mechanical scanning or optical focusing components. In QUEST, a 3 X 3 square waveguide array antenna located at the low field side is used to measure thermal emission from the overdense plasma. For the present experimental conditions, the emission frequency is expected to be in the range of 8-14 GHz, which is down converted to 70 MHz using heterodyne detection technique by a set of mixers followed by narrow band pass filters. By finding the phase matching condition for direction of arrival approach, the emission intensity and angle can be determined. Common technique for QUEST and MAST

In-situ calibration inside QUEST:

In order to find the instrument phase offset for the entire length from waveguide aperture to the detection system including signal cables, an in-situ calibration is carried out inside the QUEST vacuum chamber. A broadband noise source is installed on a three dimensional scanner in the vacuum vessel and phase evolution over propagation distance in front of each aperture is carried out by axial scanning the noise source. Such calibration is done for the entire frequency range from 8-14.5 GHz. The instrument phase offset is calibrated with reference to the port-1 of the waveguide antenna.

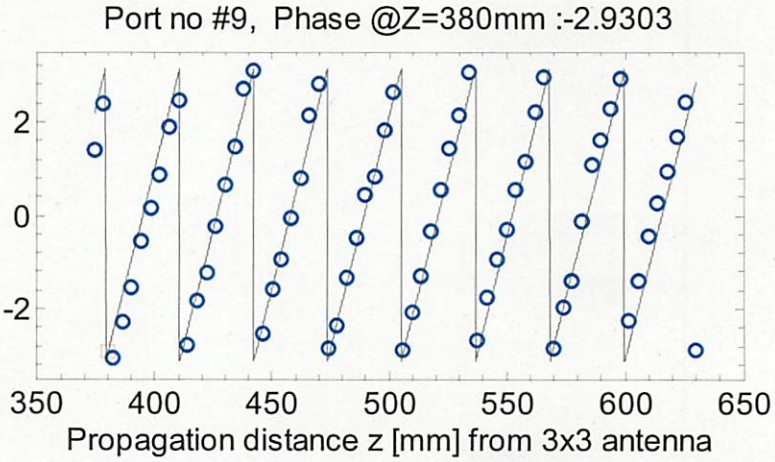

Figure-1: Typical phase evolution at 9.5 GHz as a function of propagation distance from the noise source in air.

Image reconstruction with a broadband noise source:

The broadband noise source is placed off axis in front of the receiving antenna at 9 different positions. The signals are acquired through a fast data acquisition system to record time series at 65 discrete frequencies from 8 to 14.5 GHz. The amplitude and phase are determined by least square fitting procedure and phase for each port signals are obtained. The normalized intensity is computed in the plane perpendicular to the propagation at 601 x 601 grid points by taking into account the measured phase and instrument phase offset and is shown in the figure-2. The reconstructed image is fairly matches with the actual noise source position as seen in figure-2. However, we found the presence of few side lobes with intensity < 50 % of maximum point and this can be compensated by using different adaptive beam forming techniques which is now being carried out. Similar calibration experiments are done at MAST with noise source outside the vessel and measurements of antenna array crosstalk, angular response etc. are carried out. Measured intensity patterns are modeled taking into account residual interference with adjacent passive antennae and such investigations are discussed with reference to the measurements done at QUEST experiment.

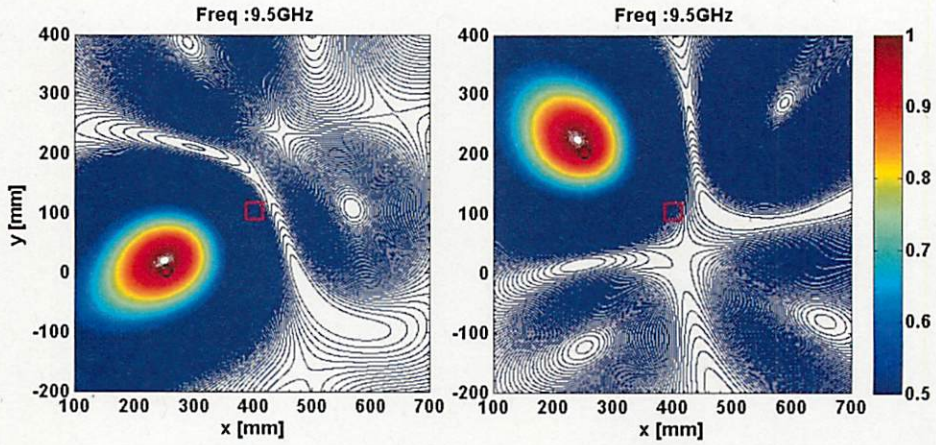

Figure-2:Noise source reconstruction from the measured phase and amplitude at waveguide antenna for two different noise source position. The red square at the centre shows the position of receiving antenna and black circle shows the physical position of the noise source. Reconstructed normalized intensity profile is shown in the contour map with color bar at right hand side.

The new DAQ system:

A new data acquisition system is being developed at QUEST for fast data acquisition and continuous data transmission with the help of Gigabit Ethernet. This will enable to improve the signal to noise ratio by signal averaging in time. In the MAST experiment, drift in signal over long time is observed in similar DAQ system and the various methods to rectify such issues is discussed in details. New set of calibration experiment with the new DAQ is proposed with noise source on the 3-dimensional scanner in QUEST vessel. Measurements with different plasma experiment will also be conducted and will be compared with the MAST results.

References:

1. H. Idei et. al., *IAEA-FEC*, **EX/P6-17**, (2012).
2. H. P. Laqua et. al., *Phy. Rev. Lett.*, **81**, 2060 (1998)
3. J. Zajac et. al., *Rev. of Scientific Instruments*, **83**, 10E327 (2012)
4. V. F. Shevchenko et. al., *JINST*, **7**, P10016 (2012)